Higher Order Structure of Chloroplastic 5S Ribosomal RNA from Spinach†

Pascale Romby,‡ Eric Westhof,‡ Rémy Toukifimpa,§ Régis Mache,§ Jean-Pierre Ebel,‡ Chantal Ehresmann,‡ and Bernard Ehresmann*,‡

Laboratoire de Biochimie, Institut de Biologie Moléculaire et Cellulaire du CNRS, 15 rue René Descartes, 67084 Strasbourg Cedex, France, and Laboratoire de Biologie Moléculaire Végétale, Université de Grenoble I, BP 68, 38402 Saint Martin d'Hères Cedex, France

Received October 8, 1987; Revised Manuscript Received December 4, 1987

ABSTRACT: The secondary and tertiary structure of chloroplastic 5S ribosomal RNA from spinach was investigated by the use of several chemical and enzymatic structure probes. The four bases were monitored at one of their Watson–Crick base-pairing positions with dimethyl sulfate [at A(N1) and C(N3)] and with 1-cyclohexyl-3-(2-morpholinoethyl)carbodiimide metho-*p*-toluenesulfonate [at G(N1) and U(N3)]. Position N7 of purines was probed with diethyl pyrocarbonate (adenines) and with dimethyl sulfate (guanines). Ethylnitrosourea was used to probe phosphate involved in tertiary interaction or in cation coordination. In order to estimate the degree of stability of helices, the various chemical reagents were employed under "native" conditions (300 mM KCl and 20 mM magnesium at 37 °C), under "semidenaturing" conditions [1 mM ethylenediaminetetraacetic acid (EDTA) at 37 °C], and under denaturing conditions (1 mM EDTA at 90 °C). Unstructured regions were also tested with single-strand-specific nucleases T_1, U_2, and S_1 and double-stranded or stacked regions with RNase V_1 from cobra *Naja naja oxiana* venom. The results confirm the existence of the five helices and the two external loops proposed in the consensus model of 5S rRNA. However, the regions depicted as unpaired internal loops appear to be folded into a more complex conformation. A three-dimensional model derived from the present data and graphic modeling for a region encompassing helix IV, helix V, loop D, and loop E (nucleotides 70–110) is proposed. Nucleotides in the so-called loop E (73–79/100–106) display unusual features: Noncanonical base pairs (A-A and A-G) are formed, and three nucleotides (C75, U78, and U105) are bulging out. This region adopts an unwound and extended conformation that can be well suited for tertiary interactions or for protein binding. Several bases and phosphates candidate for the tertiary folding of the RNA were also identified.

The 5S ribosomal RNA is a universal component of prokaryotic ribosomes and cytoplasmic ribosomes of eukaryotic cells. It is also present in chloroplastid ribosomes and in plant mitochondria. In *Escherichia coli*, it has been located in the central protuberance of the large subunit (Shatsky et al., 1980). Several functional roles have been postulated for this RNA molecule including ribosomal subunit association (Azad & Lane, 1973; Azad, 1979), tRNA binding (Brownlee et al., 1968; Ofengand & Henes, 1979), peptidyltransferase (Raacke, 1971), and GTPase (Gaunt-Klopfer & Erdmann, 1975) activities. However, despite a large body of work, the precise role of 5S rRNA in protein biosynthesis is still unknown. Further insights into the biological significance of 5S rRNA require a good understanding of its structure.

Extensive sequence comparison of 5S rRNAs led to the elaboration of a consensus secondary structure model for prokaryotes and eukaryotes [e.g., Woese and Fox (1977), Luehrsen and Fox (1981), Delihas and Andersen (1982), Delihas et al. (1984), and Erdmann and Wolters (1986)]. Both models support a highly conserved structure in the course of evolution, consistent with a common role in ribosome function. The structure of prokaryotic and eukaryotic 5S rRNA species has been partially studied by use of several enzymatic or chemical probes [e.g., Noller and Garrett (1979), Toots et al. (1981), Troutt et al. (1982), Silberklang et al. (1983), Göringer et al. (1984), Kjems et al. (1985), Digweed et al. (1986), and Sneath et al. (1986)]. Several tentative tertiary structure models have been proposed on the basis of infrared spectroscopy studies (Böhm et al., 1981), cross-linking experiments (Hancock & Wagner, 1982), enzymatic accessibility (Pieler & Erdmann, 1982), and chemical modification (McDougall & Nazar, 1986). In addition, conformational switches have been described that might be responsible for some of the discrepancies in the models proposed for the 5S rRNA structure (Kearns & Wong, 1974; Noller & Garrett, 1979; Kao & Crothers, 1980; Kime & Moore, 1982; Christensen et al., 1985). Despite a wide variety of experimental approaches, the three-dimensional arrangement of the 5S rRNA remains poorly understood, and further precise structural information is still needed.

In the present paper, the higher order structure of chloroplastic 5S rRNA from spinach was studied by using a variety of structure-specific probes and gel sequencing. Chloroplastic 5S rRNAs are known to belong to the eubacterial type. Spinach chloroplast RNA has already been shown to present similarities with *E. coli* 5S rRNA (Digweed et al., 1986), but some ambiguities still remain. Two chloroplast ribosomal proteins bind to the homologous 5S rRNA, and interestingly these proteins are different in size from the *E. coli* 5S rRNA binding proteins (unpublished results). These observations suggest that the chloroplastic 5S rRNA–protein complex would be worth studying, and therefore a detailed structure of the chloroplastic 5S rRNA has to be investigated. The present work provides a rigorous experimental test for probing the secondary and tertiary structure of the RNA at nucleotide level. A three-dimensional model that integrates these ex-

† This work was supported by grants from the Centre National de la Recherche Scientifique (CNRS) and the Ministère de la Recherche et de la Technologie (MRT).

* To whom correspondence should be addressed.
‡ Institut de Biologie Moléculaire et Cellulaire du CNRS, Strasbourg.
§ Université de Grenoble I.

0006-2960/88/0427-4721$01.50/0 Published 1988 by the American Chemical Society

perimental data was also built by graphic modeling for a region encompassing helix IV, helix V, loop D, and loop E (nucleotides 70–110).

Experimental Procedures

Buffers. Buffer A: 30 mM Tris-HCl,[1] pH 7.5, 20 mM $MgCl_2$, 300 mM KCl, and 1 mM $ZnCl_2$. Buffer B: 50 mM sodium acetate, pH 4.5, 20 mM $MgCl_2$, 300 mM KCl, and 1 mM $ZnCl_2$. Buffer C: 50 mM sodium acetate, pH 4.5, 100 mM NaCl, and 1 mM $ZnCl_2$. Buffer D: 30 mM Tris-HCl, pH 7.5, 20 mM $MgCl_2$, and 300 mM KCl. Buffer N-1: 300 mM sodium cacodylate, pH 8.0, 20 mM $MgCl_2$, and 300 mM KCl. Buffer N-1$^-$: 300 mM sodium cacodylate, pH 8.0, and 20 mM $MgCl_2$. Buffer D-1: 300 mM sodium cacodylate, pH 8.0, and 1 mM EDTA. Buffer N-2: 50 mM sodium cacodylate, pH 7.5, 20 mM $MgCl_2$, and 300 mM KCl. Buffer N-2$^-$: 50 mM sodium cacodylate, pH 7.5, and 20 mM $MgCl_2$. Buffer D-2: 50 mM sodium cacodylate, pH 7.5, and 1 mM EDTA. Buffer N-3: 50 mM sodium borate, pH 8.0, 20 mM $MgCl_2$, and 300 mM KCl. Buffer D-3: 50 mM sodium borate, pH 8.0, and 1 mM EDTA. Buffer TMK: 50 mM Tris-HCl, pH 8.3, 6 mM $MgCl_2$, and 40 mM KCl.

Chemicals and Enzymes. Aniline and CMCT were from Merck; DMS was from Aldrich Chemicals Co.; DEPC, hydrazine, and ENU were from Sigma; calf intestinal phosphatase, RNAses T_1, U_2, and V_1, nuclease S_1, and T_4 RNA ligase were from P-L Biochemicals; avian myeloblastosis reverse transcriptase was from Life Science; T_4 polynucleotide kinase, [γ-^{32}P]ATP (3200 Ci/mmol), and [5′-^{32}P]pCp (3000 Ci/mmol) were from Amersham; and acrylamide and *N*,*N*′-methylenebis(acrylamide) were from BDH Chemicals.

Preparation of Chloroplastic 5S rRNA. Spinach chloroplasts and ribosomes were isolated as previously described (Mache et al., 1980) with the following modifications. The grinding medium contained 40 mM cysteine and 4 mM EDTA. Plastids were disrupted in 10 mM Tris-HCl, pH 7.6, 5 mM dithiothreitol, 10 mM magnesium acetate, and 0.05 mM phenylmethanesulfonyl fluoride. 5S rRNA was extracted from 70S ribosomes according to the method of Dyer and Bowman (1979) and was fractionated by electrophoresis on a 10% acrylamide:0.5% bis(acrylamide):8 M urea preparative slab gel (Maxam & Gilbert, 1977).

Prior to 5′-end labeling, 5S rRNA was dephosphorylated according to the method of Shinagawa and Padmanabhan (1979), phenol extracted, and precipitated with ethanol. Labeling at the 3′-end was as described by England and Uhlenbeck (1978). The labeled 5S rRNA was purified by electrophoresis on a 10% polyacrylamide:8 M urea slab gel. The molecules were stored in the gels at −20 °C in order to minimize the degradation of the RNA. Before each experiment, the RNA was eluted, precipitated twice with ethanol, and resuspended in the adequate buffer. Renaturation of "native" 5S rRNA was as follows: the RNA was preincubated at 50 °C for 5 min and cooled slowly (30 min) at room temperature.

Limited Enzymatic Digestions of Labeled 5S rRNA. In each experiment, labeled 5S rRNA was supplemented with 1 μg of total tRNA as carrier. The digestion with nuclease S_1 was at 20 °C, either for 5 and 10 min with 50 units of enzyme in 10 μL of buffer A or for 5 and 10 min with 1 unit in 10 μL of buffer B or C. The digestions with RNAses T_1 (5×10^{-4} unit), U_2 (1 unit), and V_1 (0.05 unit) were at 20 °C for 5 and 10 min in 10 μL of buffer D. The reactions were stopped by precipitating the RNA with ethanol. Each reaction mixture (20 000 cpm Cerenkov) was subjected to electrophoresis on 15% acrylamide:0.75% bis(acrylamide):8 M urea slab gels ($30 \times 40 \times 0.05$ cm). The positions of nuclease cuts were identified by running in parallel RNases T_1 and U_2 and formamide ladders.

Alkylation of 5S rRNA by ENU. Phosphate alkylation was essentially that described by Vlassov et al. (1981). Labeled 5S rRNA was supplemented with 2 μg of tRNA as carrier. Native reaction: 5S rRNA was incubated at 20 °C for 3 h or at 37 °C for 30 min in 20 μL of buffer N-1 or Buffer N-1$^-$ with 5 μL of a ENU saturated ethanol solution. Denaturing condition: RNA was incubated at 80 °C for 2 min in 20 μL of buffer D-1 with the same amount of ENU. The reaction was stopped by ethanol precipitation. The alkylated 5S rRNA was cleaved at phosphotriester positions in 0.1 M Tris-HCl, pH 9.0, and the liberated oligonucleotides were analyzed by gel electrophoresis. The assignment of the bands was performed by running in parallel a RNAse T_1 ladder. The extent of phosphate alkylation was measured by densitometry of the autoradiographs.

Chemical Modification of the Bases. In each experiment, 5S rRNA was supplemented with 10 μg of tRNA as carrier.

DMS Modification. Native reaction: 5S rRNA was preincubated at 37 °C for 10 min in 200 μL of buffer N-2 or buffer N-2$^-$. DMS (0.5 μL) was added for an additional 5–20-min incubation with occasional stirring. Semidenaturing reaction: The same procedure as above was used except that buffer D-2 was used. Denaturing reaction: Reaction was in 250 μL of buffer D-2, and the incubation was at 90 °C for 1 min.

DEPC Modification. Native reaction: The procedure was the same, as for DMS modification but in the presence of 20 μL of DEPC for 30 min at 37 °C with occasional stirring. Semidenaturing reaction: The procedure was the same as for native conditions but in buffer D-2. Denaturing reaction: Incubation was at 90 °C for 5 min in buffer D-2 with 5 μL of DEPC.

CMCT Modification. The methodology used was derived from that described by Moazed et al. (1986). Native reaction: 5S rRNA was incubated at 37 °C for 15, 30, or 60 min in 150 μL of buffer N-3 in the presence of 50 μL of CMCT (42 mg/mL). Semidenaturing reaction: The procedure was the same as for native conditions but in 250 μL of buffer D-3 for 5 or 15 min. Denaturing reaction: The incubation was at 90 °C for 1 min in 250 μL of buffer D-3.

At the end of each incubation, 100 μL of 0.3 M sodium acetate, pH 6.0, was added, and the modified RNA was precipitated with 2.5 volumes of ethanol. Pellets were resuspended in 100 μL of 0.3 M sodium acetate, pH 6.0, precipitated with ethanol, washed with 75% ethanol, and vacuum-dried.

Detection and Analysis of the Modified Positions. Cleavage of the end-labeled 5S rRNA at modified positions [G(N7) and C(N3) with DMS, A(N7) with DEPC)] was as described by Peattie and Gilbert (1980). The liberated oligonucleotides were analyzed by electrophoresis on 15% acrylamide:0.75% bis(acrylamide):8 M urea slab gels.

The primer extension method was used to detect the bases modified by DMS [A(N1) and C(N3)] and CMCT [G(N1) and U(N3)]. The DNA primer CATCCTGGC complementary to the 3′-end of the 5S rRNA was synthesized with

[1] Abbreviations: DMS, dimethyl sulfate; CMCT, 1-cyclohexyl-3-(2-morpholinoethyl)carbodiimide metho-*p*-toluenesulfonate; DEPC, diethyl pyrocarbonate; ENU, ethylnitrosourea; RNase V_1, ribonuclease from cobra *Naja naja oxiana* venom; Tris-HCl, tris(hydroxymethyl)aminomethane hydrochloride; EDTA, ethylenediaminetetraacetic acid.

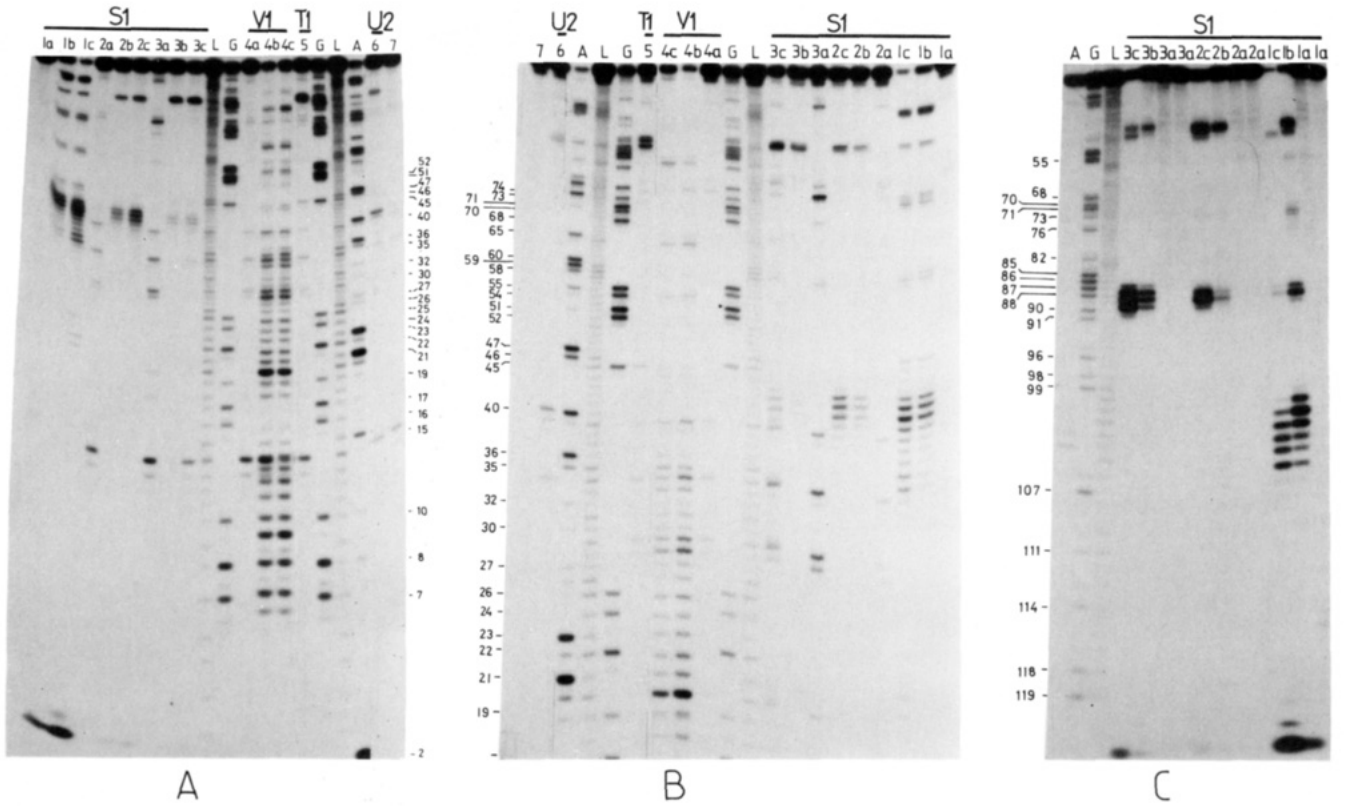

FIGURE 1: Gel electrophoresis fractionation of enzymatic digests of 5S rRNA: (A) 5′-End-labeled RNA, short migration; (B) 5′-end-labeled RNA, long migration; (C) 3′-end-labeled RNA, short migration. Nuclease S_1 in buffer C: (1a) incubation control; (1b) 5 min; (1c) 10 min. Nuclease S_1 digestion in buffer B: (2a) control; (2b) 5 min; (2c) 10 min. Nuclease S_1 in buffer A: (3a) control; (3b) 5 min; (3c) 10 min. RNase V_1 in buffer D: (4a) control; (4b) 5 min; (4c) 10 min. (5) RNase T_1, (6) RNase U_2, and (7) control in buffer D; (L) formamide, (G) RNase T_1, and (A) RNase U_2 ladders.

an Applied Biosystem apparatus using the phosphoramidite method and then labeled at its 5′-end according to the method of Silberklang et al. (1977). Hybridization of the labeled DNA primer (80 000 cpm) to the modified unlabeled 5S rRNA, primer elongation, and analysis of the generated DNA fragments were as described elsewhere (Mougel et al., 1987; Baudin et al., 1987). Occasionally, the extent of modification was measured by densitometry of the autoradiographs.

Graphic Modeling. The modeling was done with the help of several computer programs. First, on the basis of the observed chemical reactivities, a Kendrew model of loop E (i.e., residues 71–80 and 99–108) was built. The torsion angles of the sugar–phosphate backbone were measured and inserted automatically in a standard RNA helix. Corrections and rough fitting of base pairing were done manually with the interactive graphic program FRODO (Jones, 1978) adapted for the Evans and Sutherland PS 300 (Pflugrath et al., 1983). To ensure proper geometry for base pairing and correct stereochemistry, the output of FRODO was subjected to Hendrickson–Konnert restrained least squares (Konnert & Hendrickson, 1980) with the programs NUCLIN and NUCLSQ (Westhof et al., 1985). The structure was then introduced in the energy minimization program AMBER (Weiner & Kollman, 1981). Helices IV and V were built as standard RNA helices by using the program NAHELIX. Modeling of loop D was accomplished with the program FRAGMENT, which inserts any base sequence on a substructure chosen in a data base. The various fragments were hooked together interactively with the program FRODO and subjected to least-squares and energy minimization. Details of the various programs will be given elsewhere.

RESULTS

Accessibility of 5S rRNA to Nucleases. The conformation of chloroplastic 5S rRNA has been tested with single-strand-specific nucleases (T_1, U_2, S_1) and with RNase V_1 specific for structured regions. Enzymatic cleavages were introduced at a low yield so that statistically less than one cut per molecule occurred. In order to test the possible formation of secondary cuts that may not reflect the native conformation of the RNA, the 5S rRNA has been probed on both 5′- and 3′-end-labeled molecules. Since the same hydrolysis pattern was obtained from both end-labeled molecules, it could be deduced that all of the observed cuts were primary cuts. The native conformation of the RNA was tested with all enzymes at neutral pH in the presence of magnesium and KCl. As the pH used in our experiments is rather far from the optimal pH for nuclease S1 (pH 4.5), special care was necessary for the use of this nuclease. Since discrete conformational changes can be induced by different pH and salt conditions, the digestion pattern of nuclease S_1 obtained in the above-mentioned conditions was compared to that obtained by others at pH 4.5, either in the absence of magnesium (Pieler et al., 1983) or in the presence of magnesium.

For convenience, enzymatic cuts will be designated by the position in the sequence of the nucleotide directly located at the 5′-side of the scission. Typical experiments are shown in Figure 1, and the results are summarized in Figure 2. With RNases T_1 and U_2, purines 40 and 87–91 are by far the most accessible, whereas G45 is also cut but to a very low extent (Figure 1B, lanes 5,6). Regarding the accessibility to nuclease S_1, two major series of cuts are observed at pH 7.5 in the presence of magnesium (buffer A) in regions 39–41 and 86–89 (Figure 1, lane 3b,c). It is also apparent that both extremities of the RNA are accessible. Under the conditions described by Pieler et al. (1983) (buffer C, pH 4.5, in the absence of magnesium), additional cuts appear in regions 34–46, 56–58,

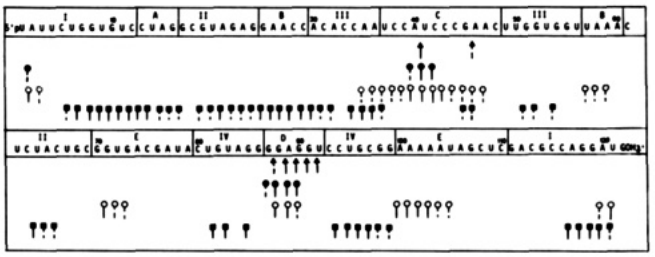

FIGURE 2: Schematic representation of the accessibility of 5S rRNA to nucleases. Cleavages are represented by arrows with different heads: (▲) RNases T_1 and U_2 and (●) nuclease S_1 in buffer A (pH 7.5, magnesium); (○) nuclease S_1 in buffer C (pH 4.5, absence of magnesium); (■) RNase V_1 in buffer D. A full line indicates a strong hit, and a dotted line indicates a weak hit. The figure represents a summary of results in Figure 1 and of three other distinct experiments.

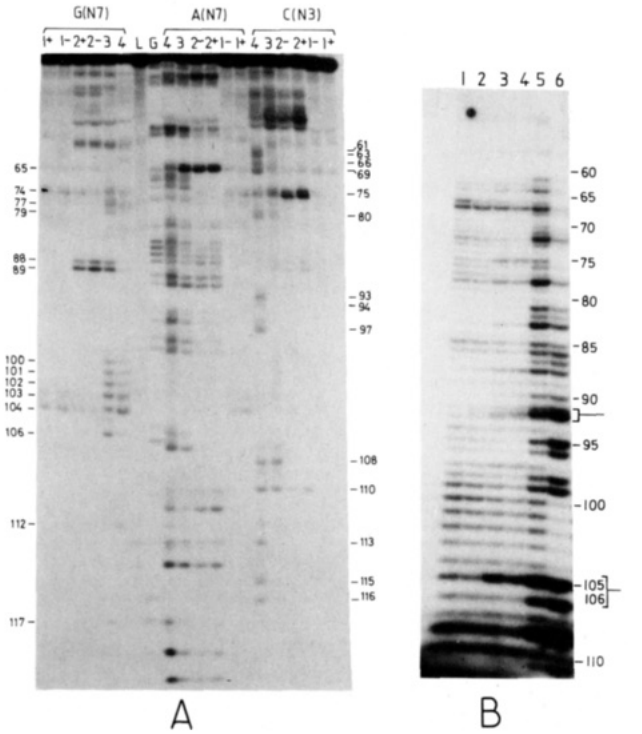

FIGURE 3: (A) Gel fractionation of 3′-end-labeled 5S rRNA after cleavage at the modified nucleotides with DMS [C(N3) and G(N7)] and DEPC [A(N7)]. Incubation in buffer N-2 or N-2⁻ (native conditions): (1) control; (2) reactions at G(N7) for 10 min, at A(N7) for 30 min, at C(N3) for 20 min. Incubation in buffer D-2 (semidenaturing conditions): (3) reactions at G(N7) for 5 min, at A(N7) for 30 min, at C(N3) for 10 min. Incubation in buffer D-2 (denaturating conditions): (4). The presence or absence of KCl is denoted by + or −. Formamide (L) and RNase T_1 (G) ladders are indicated. (B) Gel electrophoresis fractionation of 5S rRNA modified with CMCT [G(N1) and U(N3)]. Detection was by primer extension. Incubation in buffer N-3 (native conditions): (1) control; (2) 15 min; (3) 30 min; (4) 60 min. Incubation in buffer D-3: (5) semi-denaturing conditions; and (6) denaturing conditions. Band compression is indicated by square brackets. For one experiment, several gel electrophoresis migrations were done to analyze the complete 5S rRNA molecule.

70–73, and 99–104 (see Figure 1, lane 1b,c). However, when magnesium was added at pH 4.5 (buffer B), the hydrolysis pattern was close to that obtained under standard conditions. RNase V_1 hydrolysis patterns allowed us to locate cleavages at positions 5–16, 18–31, 33–36, 44–45, 50–51, 53, 63–65,81–82, 84, 93–98, and 116–120 (Figures 1A,B and 2).

Reactivity of 5S rRNA to Chemical Probes. Two approaches were used to identify nucleotides reacting with the different chemical structure probes. The first one allowed mapping of the reactivity of C(N3) and G(N7) to DMS, of A(N7) to DEPC, and of phosphates to ENU after appropriate

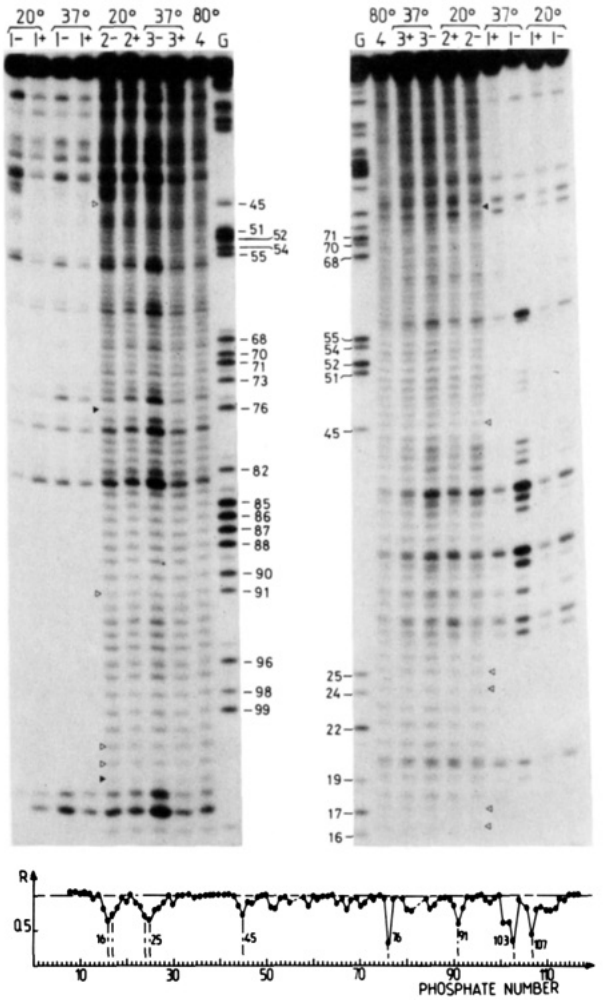

FIGURE 4: Gel electrophoresis fractionation of 3′-end-labeled (A) and 5′-end-labeled (B) 5S RNA treated with ENU. Incubation in buffer N-1 or N-1⁻ (1) control; (2) 3 h at 20 °C; (3) 30 min at 37 °C. Incubation in buffer D-1; (4) 2 min at 80 °C. (C) Pattern of phosphate reactivities to ENU in native conditions vs denaturated conditions. *R* values are the ratios between the intensities of the corresponding bands in both conditions. These intensities were measured as peak heights on the densitograms of the gels. A ratio $R < 1$ means that alkylation of a given phosphate is lower in the native molecule than in the unfolded one. The reactivity of some phosphates that could not be analyzed due to unspecific degradations are indicated by a dotted line.

cleavage reaction on both 5′- and 3′-end-labeled 5S rRNA. Typical examples are given in Figure 3A for DMS and DEPC and in Figure 4 for ENU. Spontaneous cleavages occurring essentially at pyrimidine–adenine sequences are observed in the incubation control. This has already been shown in other RNA molecules (Carbon et al., 1978; Florentz et al., 1982; Romby et al., 1985; Moazed et al., 1986). These cuts are not induced by contaminating nucleases but are thought to reflect an intrinsic chemical instability partly based on a particular flexibility and on a specific environment at those positions leading to an alkaline-type hydrolysis (Brown, 1974; Moras et al., 1983). In the second approach, unlabeled RNA was submitted to chemical modification. The modified RNA was then used as a template for extension of a 5′-labeled synthetic oligodeoxyribonucleotide complementary to the 3′-end of the RNA using reverse transcriptase and the four dNTPs. Modification at Watson–Crick positions stops the progress of reverse transcription and yields prematurely terminated DNA fragments. This technique allowed probing of each base at one of its Watson–Crick positions by use of DMS for A(N1) and C(N3) and of CMCT for G(N1) and U(N3). Typical

experiments are shown in Figure 3B. Artifact bands can be observed in incubation controls, which sometimes make the interpretation of the autoradiograph difficult. This is particularly the case of nucleotides 101–107 that are close to the priming site used for reverse transcriptase. To evaluate the degree of reactivity of residues, the lanes of the autoradiograph corresponding to the incubation control and to the reactions under native and semidenaturing conditions were scanned. After standardization, the values corresponding to the different bands in the control lane were subtracted from those in the reaction lanes. Since only a few minor cuts in the RNA chain were evidenced in end-labeled RNA, a likely explanation for these stops or pauses is the difficulty for reverse transcriptase to melt certain particularly structured regions, especially because transcription is done in the presence of magnesium. Despite this difficulty, primer extension remains the only methodology to map A(N1), G(N1), and U(N3), for which no chemical reaction is known to induce cleavage at the modified residue. As far as the reactivity of bases is concerned, it should be kept in mind that C(N3) reacts slower than A(N1) to DMS and G(N1) slower than U(N3) to CMCT.

The reactivity of bases and phosphates to the various chemical probes is illustrated on the consensus secondary structure model of the chloroplastic 5S rRNA (Figure 5). All of the experiments have been repeated 3 times with a satisfying reproducibility. Reactivity to DMS, DEPC, and CMCT was tested under native (in the presence or absence of KCl), semidenaturing, and denaturing conditions. Phosphates were tested with ENU under native (at 20 and 37 °C) and denaturing conditions.

Under native conditions, several phosphates (positions 76, 103, 107) have a strongly reduced reactivity (more than 50%) toward ENU as compared to denaturing conditions (Figure 4B). In addition, the reactivity of phosphates 16, 17, 24, 25, 45, 101, and 102 is moderately reduced (25–45%). Some of these reductions are within the limit of experimental error. Nevertheless, we think that they are significant, since they were reproducibly observed in several independent experiments. The reactivity toward DMS, CMCT, and DEPC was found to be dependent on the buffer conditions. Under native conditions (presence of magnesium, 37 °C), a number of nucleotides involved in hydrogen bonding are unreactive. The presence or absence of KCl in the incubation buffer was found to have no effect on the reactivity pattern (see Figure 3). Under semidenaturing conditions (absence of magnesium, 37 °C), several bases unreactive under native conditions became reactive, thus confirming the crucial role played by magnesium in the folding of the RNA. As far as Watson–Crick base-pairing positions are concerned (see Figure 5A), those positions that become reactive under semidenaturing conditions are primarily located in helices. More interesting are those positions located in loops that are unreactive under native conditions and reactive under semidenaturing conditions. Those positions, not involved in the secondary folding, most likely participate in tertiary interactions.

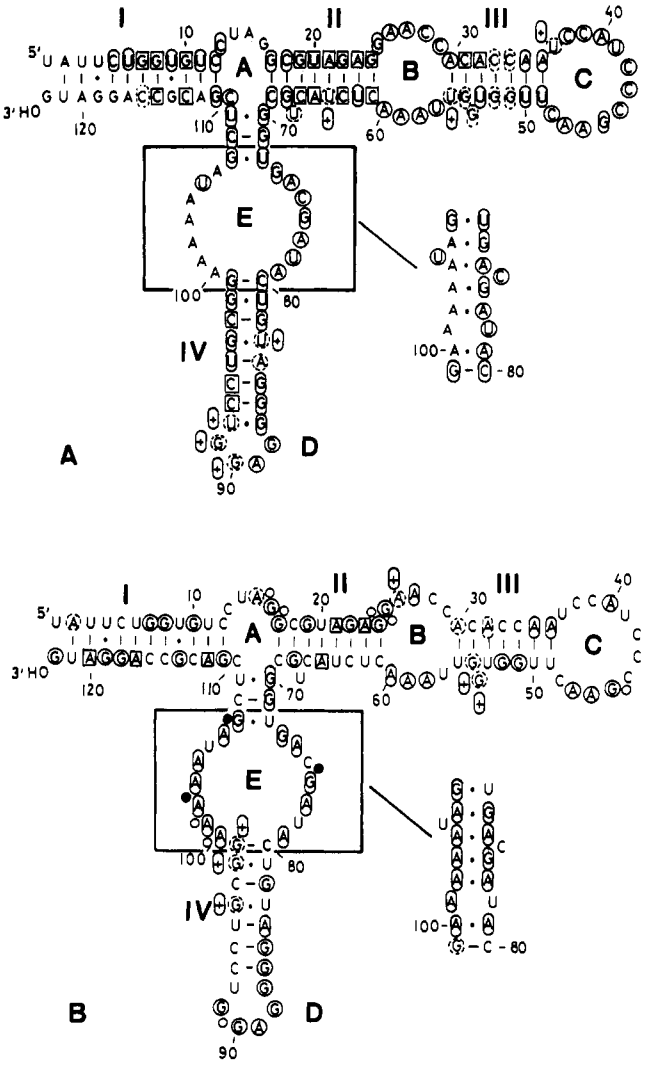

FIGURE 5: Summary of the reactivities of 5S rRNA to the different chemical probes on the concensus secondary structure model. A possible base-pairing scheme for the boxed region is shown as an inset. (A) Reactivity of Watson–Crick positions (N1 of purines and N3 of pyrimidines): (○) reactive under native conditions; (◌) unreactive under native conditions but reactive under semidenaturing conditions; (□) reactive only under denaturing conditions. Symbols in dotted lines represent marginal reactivities. The increase of reactivities under semidenaturing conditions, as compared to the native ones, is denoted by ⊕. (B) Reactivities of position N7 of purines and of phosphates. The reactivity of position N7 of purines is indicated as above for native, semidenaturing, and denaturing conditions. Unreactive phosphates in native conditions are denoted by a full circle, and partial reactivity is denoted by an empty circle.

Discussion

Discussion will be conducted separately for region 1–69/111–122 (containing helices I, II, and III and loops A, B, and C) and for region 70–110 (containing helices IV and V and loops D and E).

Region 1–69/111–122. The existence of helices I–III is clearly demonstrated by the nonreactivity at Watson–Crick positions under native conditions and by the presence of RNase V_1 cuts (Figure 2). Only the two extremities of helix I are cut by nuclease S_1. Helix II is the most stable, although a marginal reactivity could be observed at U64. In helix III, most of the residues become reactive under semidenaturing conditions. Also in the absence of magnesium, several nuclease S_1 cuts appear in this helix. This weak stability can be correlated with the high content in A–U base pairs. Phylogenetic conservation shows that in 5S rRNA the first two base pairs A30–U56 and C31–G55 in helix III are highly conserved. In all chloroplastic 5S rRNAs, helix III contains seven base pairs with a bulged guanine residue at position 54. The nonreactivity of G54(N1) suggests that this residue is stacked inside the helix between residues U53 and G55, introducing an irregularity in the helix. The terminal base pair A30–U56 presents a moderate reactivity at Watson–Crick positions. It has already been reported in *E. coli* 16S rRNA that reactivity is often observed in terminal A–U base pairs located at the junction of internal loops (Baudin et al., 1987). This reactivity may result from an increased flexibility in these particular regions.

However, another possibility that is well correlated with the observed chemical reactivities can be proposed for the chloroplastic 5S rRNA. It involves a noncanonical base pairing between A30(N7,N6) in a syn conformation and G55(N1,06) in an anti conformation and a Watson–Crick base pairing between C31 and G54. Such an A–G base pair was found in the crystal structure of a DNA dodecamer (Hunter et al., 1986). It was also proposed to occur in ribosomal RNAs (Traub & Sussman, 1982). Indeed, these authors observed that potential A–G base pairs are often located at the end of a double-helical region in ribosomal RNAs.

Loop C is a well-defined external 12-base loop. All nucleotides in this loop are remarkably conserved through evolution (Wolters & Erdmann, 1984; Delihas et al., 1984; Erdmann & Wolters, 1986). All residues exhibit a strong reactivity at Watson–Crick positions, with the exception of U37 and G45. Purines are also reactive at their N7 position, indicating that these residues are fully exposed. Cleavages produced by nucleases T_1, U_2, and S_1 are observed in this loop. Note that two minor RNase V_1 cuts are located between nucleotides 44 and 45 and that phosphate 45 exhibits a lower reactivity, while G45 is unreactive at position N1. This suggests that residue 45 is involved in a tertiary interaction. Two Watson–Crick base pairs, C38–G45 and U39–A46, have been proposed in wheat germ 5S rRNA (Li et al., 1987). In chloroplastic 5S rRNA, the high reactivity of C38(N3) and A46(N1) does not support such interactions. However, a local tertiary interaction between U37 and G45 may occur. In loop B, all bases are fully reactive at Watson–Crick positions, with the exception of G25. Several RNase V_1 cuts are observed on the 5′-side of the loop, while no nuclease S_1 cuts are present. All purines are reactive at their N7 position, with the exception of A27 and A60. Two possible interpretations can be invoked for the nonreactivity of G25(N1): (i) a noncanonical base between G25 and A60 involving two hydrogen bonds between G(N1, O6) and A(N7, N6) [supported by the nonreactivity of A60(N7)]; (ii) a tertiary long-range interaction between G25 and some unidentified residue, A60(N7) being protected due to stacking. The presence of a magnesium binding site in this area is supported by the decreased reactivity of the two adjacent phosphates 24 and 25. In loop A, Watson–Crick positions of every base could not be easily investigated due to the presence of numerous pauses or stops of reverse transcription. Nevertheless, C13(N3) clearly appears unreactive, and phosphates 16 and 17 have been found to have a reduced reactivity (Figure 5). No accessibility to single-stranded nucleases is observed, while several RNase V_1 cuts are produced. The fact that RNase V_1 cleavages are found all along helix I, helix II, loop A, and loop B suggests that helices I and II are coaxial. Loop A should be in a continuous helical structure between helices I and II.

Region 70–110. Helices IV and V are confirmed by the nonreactivity at Watson–Crick positions under native conditions. Most nucleotides become reactive under semidenaturing conditions. This weak stability can be correlated with the presence of several G–U base pairs. Nuclease S_1 cuts, which appear at positions 70–72 in the absence of magnesium, would result from the melting of helix IV. Marginal reactivity of U83(N3) and A84(N1) is noted in helix V, which may result from an increased flexibility in this particular region. It has been shown that internal (G-U/A-U)-rich stretches in helices exhibit dynamic premelting properties (Pieler et al., 1985). Helix V is accessible to RNase V_1, while no cuts are observed in helix IV. This lack of cleavage can be correlated to the fact that the minimum size of the RNA substrates is four to six base pairs in a regular helix (Lowman & Draper, 1986) or is due to steric hindrance.

Loop D is a well-defined exterior loop. Strong cleavages produced by single-strand-specific enzymes are observed, and both G88 and A89 are fully reactive at positions N1 and N7. Nevertheless, G90 and G91 exhibit a low reactivity at their position N1. Also, phosphate 91 presents a low reactivity toward ENU. In loop E, nucleotides 73–79 and 100–106 do not appear to be involved in Watson–Crick interactions, with the exception of G73 and G76. However, none of the single-strand-specific enzymes cleaves in loop E under native conditions, while the absence of magnesium induces nuclease S_1 cuts on both sides of this region. Finally, all the purines are unreactive at position N7 under native conditions and become reactive when magnesium is withdrawn. In a purine-rich single strand, one could expect that the position N7 would be protected by stacking with the Watson–Crick positions fully accessible. Following this idea, loop E would consist of two separated single strands without hydrogen bonds between them, even when complementary bases are facing each other (e.g., A74–U105), and without bad van der Waals contacts between noncomplementary bases. We found it difficult to arrive at a meaningful model on these principles. Furthermore, such a model would not explain the importance of magnesium for the stability and the protection of the phosphates. Another possibility would consist in swinging out the bases with the sugar–phosphate backbone toward the interior. However, in such a structure the N7 of purines are reactive (e.g., the interior loop 607–611/629–631 in 16S rRNA; Mougel et al., 1987). Thus, the experimental observations rather suggest that what has been defined as a symmetrical internal loop in the conventional structure model may in fact correspond to a more complex structure. Interior loops are structural elements frequently found in ribosomal RNAs. They are often rich in adenine residues. As yet, relatively little is known about the tertiary folding of such structures. In order to go further in the comprehension of the fine structure of such an interior loop, a three-dimensional model of region 70–110 was built by using graphic modeling. Stereoscopic views of this region are shown in Figures 6 and 7. This model integrates the present experimental data and known stereochemical constraints.

Helices IV and V were constructed as regular A-helices. The four-base loop D was modeled on residues 33–36 of an anticodon loop, with G88 occupying the "U-turn" at position 33 (see Figure 6). The construction leads to a 3′-stacking between A89, G90, and G91 and helix IV. This explains the low reactivity of the two guanines at position N1. Another possible explanation might be the presence of a magnesium binding site in the loop as in the crystallographic structure of yeast $tRNA^{Phe}$ [e.g., Rich et al. (1977)]. In our model, G88(N2) interacts through a hydrogen bond with phosphate 91 (Figure 6). Note that this phosphate is only partially reactive to ENU.

In region E, the postulated structure is based on several unusual A–A and A–G base pairs. The A–A pair is based on two hydrogen bonds between A(N6, N7) and A(N7, N6). This pairing has already been observed in the crystallographic structures of yeast $tRNA^{Phe}$ and $tRNA^{Asp}$ (Rich et al., 1977; Westhof et al., 1985). However, in the present case one adenine of each A–A pair adopts the syn conformation around its glycosyl bond. This can be correlated to the nonreactivity of adenines 74, 77, 79, 100–104, and 106 at position N7 and with their reactivity at position N1. The construction of A79–A100 and A77–A102 pairs imposes a structural con-

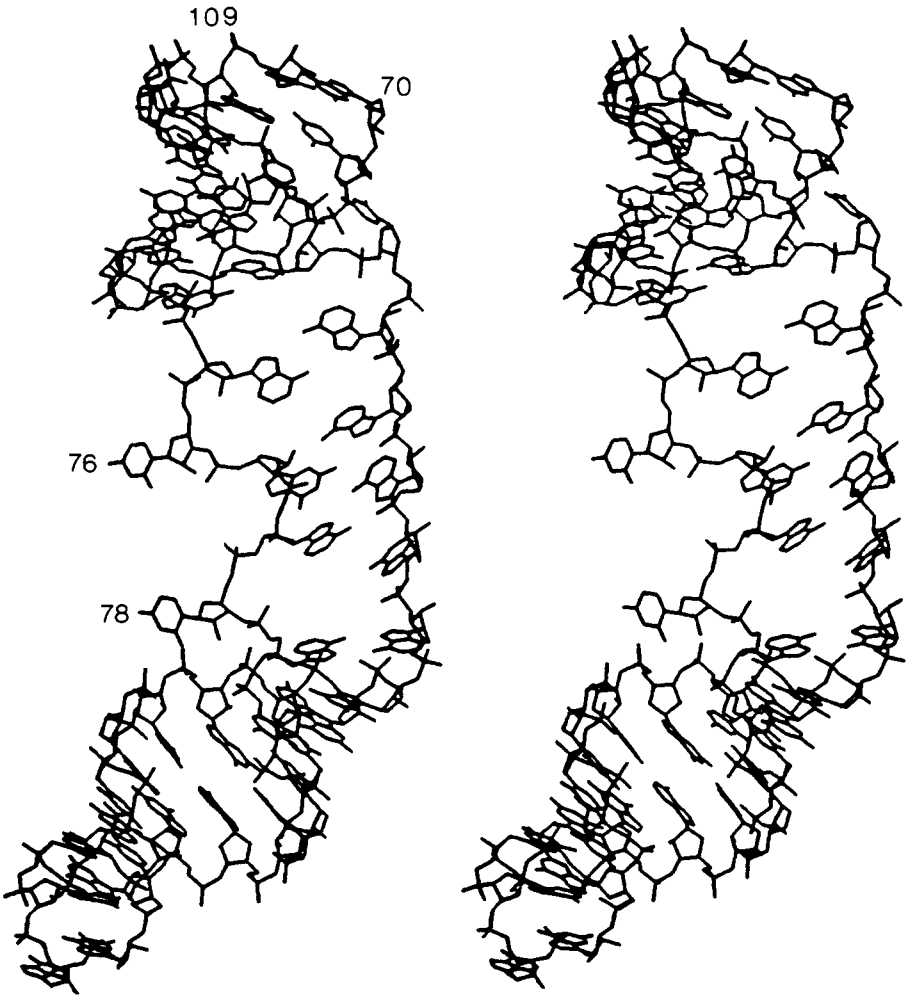

FIGURE 6: Stereoscopic view of the three-dimensional model proposed for nucleotides 70–109.

straint that does not allow a Watson–Crick base pairing between U78 and A101. In the model, U78 is bulging out and A101 is stacked between A100 and A102 (Figure 7). The observed reactivities of U78(N3) and A101(N1) and the nonreactivity of A101(N7) are in agreement with the model. The existence of A–G base pairing in 5S rRNAs has already been proposed by several authors (Stahl et al., 1981; Traub & Sussman, 1982; Delihas et al., 1984; Andersen et al., 1984; Kjems et al., 1985). In our modeling, we used two types of A–G base pairs. The first type involves two hydrogen bonds between A(N6, N7) in a syn conformation and G(O6, N1) in an anti conformation (Figure 7a); the second one involves A(N6, N7) and G(N3, N2), both in an anti conformation (Figure 7b). The two postulated A–G pairs appear as the best possibilities with respect to both internal constraints and the constraints imposed by the two adjacent helices. In each model, the two A–G base pairs are of the same type, although it is difficult to exclude a model with a different type for each A–G pair. The pair A(N6, N7)–G(O6, N1) is the same pair as that proposed in helix III. For the A(N7, N6)–G(N3, N2) pair, the closest pair was found in the structure of dCpG (Cruse et al., 1983), where two guanines form intermolecular hydrogen bonds through their N3 and N2 atoms. The chemical reactivities support the A(N7, N6)–G(N1, O6) pairing rather than the second possibility. The existence of G73–A106, A74–A104, and G76–A103 pairs imposes a structural constraint so that C75 and U105 are in a bulged out conformation. This can be correlated to the high reactivity at their position N3. In the two models, it appears that the two RNA strands do not display the feature of a standard A-helix but rather adopt an unwound and extended configuration (Figures 6 and 7). Such a conformation would favor the possibility of long-range interactions or of protein binding. However, the nonreactivity of position N7 of G73 and G76 cannot be explained in a straightforward way by the two models. For G73, one could invoke stacking and for G76 an interaction between A77(O2′), phosphate 76, and a magnesium ion. Another possible explanation is that these positions, which are exposed in the proposed model, are engaged in long-range tertiary interactions.

The nonreactivity of phosphates 76 and 107 might be explained by the assumption of cation binding (such as magnesium), resulting in "ion shielding" as discussed for tRNA (Vlassov et al., 1981; Romby et al., 1985). It is noteworthy that these phosphates were also found protected in other 5S rRNAs (McDougall & Nazar, 1986). The configuration of phosphates in our model is consistent with the existence of such a coordination site that could help to stabilize this unusual backbone folding. This has already been proposed for ribosomal protein S8 binding site in 16S rRNA, where several phosphates have been found protected in the irregular part of the helix (Mougel et al., 1987). The nonreactivity of phosphates 101–103 cannot be clearly explained. A possible interaction with the position N6 of the opposite adenines can occur (Figure 7).

CONCLUSION

By the combined use of a variety of probing strategies, it was possible to probe almost every base and phosphate in the molecule and to gain a detailed insight into the precise in-

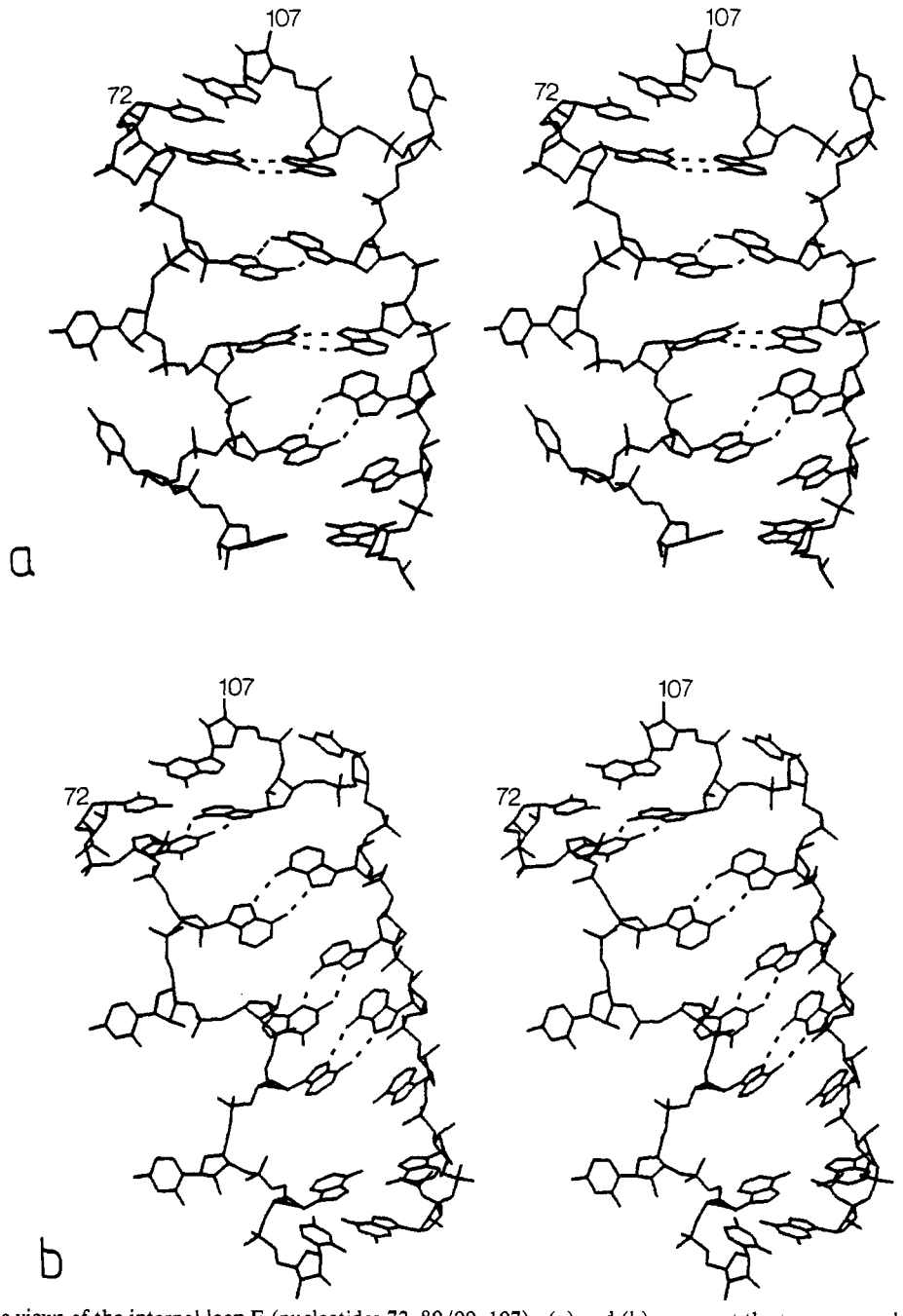

FIGURE 7: Stereoscopic views of the internal loop E (nucleotides 72–80/99–107). (a) and (b) represent the two proposed models with different A–G base pairs: (a) G(06, N1)–A(N6, N7); (b) G(N3, N2)–A(N6, N7).

volvement of nucleotides in the higher order structure. Combining experimental data resulting from structure probing and specific information collected from the known crystallographic structures of tRNAs, it has been possible to construct a three-dimensional model for region 70–110. This segment comprises one exterior four-base loop (D) and two regular A-helices (IV and V) interrupted by a region displaying unusual features (E). Noncanonical base pairs (A–A and A–G) in this particular region result in a distorted helix. Regarding modeling of the complete 5S rRNA structure, more experimental data are required. Several tentative tertiary structure models have been proposed, essentially for *E. coli* 5S rRNA, which would bring loops C and E in close proximity. Base pairs have been proposed between residues 41–44 and 74–77 (Pieler & Erdmann, 1982) or between 37–40 and either 73–76 (Hancock & Wagner, 1982) or 75–78 (Böhm et al., 1981). A pseudoknotted structure has been proposed between helix III and loop A (Göringer & Wagner, 1986). In the spinach chloroplast 5S rRNA, a tertiary interaction between 43C-C-G45 and 70G-G-U72 had been postulated (Pieler et al., 1983). However, from our results and in agreement with the consensus secondary structure model, 70G-G-U72 is base-paired with 107G-C-U109 rather than with 43C-C-G45, forming helix IV (see Figure 5). In this study, we have detected several bases and phosphates that display unexpected reactivities. Most of these cases are discussed in the present paper. However, it is presently difficult to distinguish whether these nucleotides are involved in a local tertiary interactions or in long-term interactions. Remarkably, these nucleotides are highly conserved throughout evolution and are certainly essential for the folding of the RNA molecule. Further experimental evidence, such as directed mutagenesis of 5S rRNA and the study of the 5S rRNA–protein interactions, will help in the comprehension of the exact nature of the tertiary interactions.

ACKNOWLEDGMENTS

We are indebted to J. Colin for the synthesis of the oligodeoxyribonucleotide, to F. Eyermann for skillful technical assistance, to M. Mougel and C. Rozier for helpful discussions, and to Y. Boulanger for critical reading of the manuscript. The graphic modeling has been done on the PS 300 of the laboratory of Molecular Cristallography (IBMC, Strasbourg). We thank Dr. D. Moras for making it available and for his constant interest.

REFERENCES

Andersen, J., Delihas, N., Hanas, J. S., & Wu, C. W. (1984) *Biochemistry 23*, 5759–5766.

Azad, A. A. (1979) *Nucleic Acids Res. 7*, 1913–1929.

Azad, A. A., & Lane, B. G. (1973) *Can. J. Biochem. 51*, 1669–1672.

Baudin, F., Ehresmann, C., Romby, P., Mougel, M., Lempereur, L., Bachellerie, J. P., Ebel, J. P., & Ehresmann, B. (1987) *Biochimie 69*, 1081–1096.

Böhm, S., Fabian, H., Venyaninov, S. Y., Matveer, S. V., Lucius, H., Welfe, H., & Filimonov, V. V. (1981) *FEBS Lett. 132*, 357–361.

Brown, D. M. (1974) in *Basic Principles in Nucleic Acids Chemistry* (Ts'o, P.O.P., Ed.) pp 1–90, Academic, New York.

Brownlee, G. G., Sanger, F., & Barrel, B. G. (1968) *J. Mol. Biol. 34*, 379–386.

Carbon, P., Ehresmann, C., Ehresmann, B., & Ebel, J. P. (1978) *FEBS Lett. 94*, 152–156.

Christensen, A., Mathiesen, M., Peattie, D., & Garrett, R. A. (1985) *Biochemistry 24*, 2284–2291.

Cruse, W. B. J., Egert, E., Kennard, O., Sala, G. B., Salisbury, S. A., & Viswamitra, M. A. (1983) *Biochemistry 22*, 1833–1839.

Delihas, N., & Andersen, J. (1982) *Nucleic Acids Res. 10*, 7323–7343.

Delihas, N., Andersen, J., & Singhal, R. P. (1984) *Prog. Nucleic Acid Res. Mol. Biol. 31*, 161–190.

Digweed, M., Pieler, T., Kluwe, D., Schuster, L., Walker, R. & Erdmann, V. A. (1986) *Eur. J. Biochem. 154*, 31–39.

Dyer, T. A., & Bowman, C. M. (1979) *Biochem. J. 183*, 595–604.

England, T. E., & Uhlenbeck, O. C. (1978) *Nature (London) 275*, 560–604.

Erdmann, V. A., & Wolters, J. (1986) *Nucleic Acids Res. 14*, r1–r59.

Florentz, C., Briand, J. P., Romby, P., Hirth, L., Ebel, J. P., & Giegé, R. (1982) *EMBO J. 1*, 269–276.

Gaunt-Klopfer, M., & Erdmann, V. A. (1975) *Biochim. Biophys. Acta 390*, 226–230.

Göringer, H. U., & Wagner, R. (1986) *Nucleic Acids Res. 14*, 7473–7485.

Göringer, H. U., Szymkowiak, C., & Wagner, R. (1984) *Eur. J. Biochem. 144*, 22–34.

Hancock, J., & Wagner, R. (1982) *Nucleic Acids Res. 10*, 1257–1269.

Hunter, W. N., Brown, T., & Kennard, O. (1986) *J. Biomol. Struct. Dyn. 4*, 173–191.

Jones, A. (1978) *J. Appl. Crystallogr. 11*, 268–278.

Kao, T. M., & Crothers, D. M. (1980) *Proc. Natl. Acad. Sci. U.S.A. 77*, 3360–3364.

Kearns, D. R., & Wong, Y. P. (1974) *J. Mol. Biol. 87*, 755–774.

Kime, M. J., & Moore, P. B. (1982) *Nucleic Acids Res. 10*, 4973–4983.

Kjems, J., Olesen, S. E., & Garrett, R. A. (1985) *Biochemistry 24*, 241–250.

Konnert, J. H., & Hendrickson, W. A. (1980) *Acta Crystallogr., Sect. A: Cryst. Phys., Diffr., Theor. Gen. Crystallogr. A36*, 344–349.

Li, S. J., Wu, J., & Marschall, A. G. (1987) *Biochemistry 26*, 1578–1585.

Lowman, H. B., & Draper, D. E. (1986) *J. Biol. Chem. 261*, 5396–5403.

Luehrsen, K. E., & Fox, G. E. (1981) *Proc. Natl. Acad. Sci. U.S.A. 78*, 2150–2154.

Mache, R., Dorne, A. M., & Marti-Battle, R. (1980) *MGG, Mol. Gen. Genet. 177*, 333–338.

Maxam, A. M., & Gilbert, W. (1977) *Proc. Natl. Acad. Sci U.S.A. 74*, 560–564.

McDougall, J., & Nazar, R. N. (1986) *Nucleic Acids Res. 15*, 161–179.

Moazed, D., Stern, S., & Noller, H. F. (1986) *J. Mol. Biol. 187*, 399–416.

Moras, D., Dock, A. C., Dumas, P., Westhof, E., Romby, P., & Giegé, R. (1983) in *Nucleic Acids: The Vector of Life* (Pullman, B., & Jortner, J., Eds.) Vol. 16, pp 403–411, Reidel, Dordrecht, The Netherlands.

Mougel, M., Eyermann, F., Westhof, E., Romby, P., Expert-Bezançon, A., Ebel, J. P., Ehresmann, B., & Ehresmann, C. (1987) *J. Mol. Biol. 198*, 91–107.

Noller, H. F., & Garrett, R. A. (1979) *J. Mol. Biol. 132*, 621–636.

Ofengand, J., & Henes, C. (1979) *J. Biol. Chem. 244*, 6241–6253.

Peattie, D. A., & Gilbert, W. (1980) *Proc. Natl. Acad. Sci. U.S.A. 77*, 4679–4682.

Peattie, D. A., Douthwaite, S., Garrett, R. A., & Noller, H. F. (1981) *Proc. Natl. Acad. Sci. U.S.A. 78*, 7331–7335.

Pflugrath, J. W., Saper, M. A., & Quiocho, F. A. (1983) *J. Mol. Graphics 1*, 53–56.

Pieler, T., & Erdmann, V. A. (1982) *Proc. Natl. Acad. Sci. U.S.A. 79*, 4599–4603.

Pieler, T., Digweed, M., Bartsch, M., & Erdmann, V. A. (1983) *Nucleic Acids Res. 11*, 591–604.

Pieler, T., Digweed, M., & Erdmann, V. A. (1985) *J. Biomol. Struct. Dyn. 3*, 495–514.

Raacke, I. D. (1971) *Proc. Natl. Acad. Sci. U.S.A. 68*, 2357–2360.

Rich, A. (1977) *Acc. Chem. Res. 10*, 388–396.

Romby, P., Moras, D., Bergdoll, M., Dumas, P., Vlassov, V. V., Westhof, E., Ebel, J. P., & Giegé, R. (1985) *J. Mol. Biol. 184*, 455–471.

Shatsky, I. N., Evstafieva, A. G., Bystrova, A. A., Bogdanov, A. A., & Vassiliev, V. D. (1980) *FEBS Lett. 121*, 97–100.

Shinagawa, M., & Padmanabhan, R. (1979) *Anal. Biochem. 95*, 458–464.

Silberklang, M., Gillam, A. M., & RajBhandary, U. L. (1977) *Nucleic Acids Res. 4*, 4091–4108.

Silberklang, M., RajBhandary, U. L., Lück, A., & Erdmann, V. A. (1983) *Nucleic Acids Res. 11*, 605–617.

Sneath, B., Vary, C., Pavlakis, G., & Vournakis, J. (1986) *Nucleic Acids Res. 14*, 1365–1378.

Stahl, D. A., Luehrsen, K. R., Woese, C. R., & Pace, N. R. (1981) *Nucleic Acids Res. 9*, 6129–6137.

Toots, I., Metspalu, A., & Saarma, M. (1981) *Nucleic Acids Res. 9*, 5331–5343.

Traub, W., & Sussman, J. (1982) *Nucleic Acids Res. 10*, 2701–2708.

Troutt, A., Savin, T., Curtis, W. C., Celentano, J., & Vournakis, J. (1982) *Nucleic Acids Res. 10*, 653-663.
Vlassov, V. V., Giegé, R., & Ebel, J. P. (1981) *Eur. J. Biochem. 119*, 51-59.
Weiner, P. K., & Kollman, P. A. (1981) *J. Comput. Chem. 2*, 287-293.
Westhof, E., Dumas, P., & Moras, D. (1985) *J. Mol. Biol. 184*, 119-145.
Woese, C. R., & Fox, G. E. (1977) *Proc. Natl. Acad. Sci. U.S.A. 74*, 5088-5092.
Wolters, J., & Erdmann, V. A. (1984) *Endocyt. C. Res. 1*, 1-23.

Enhanced DNA Repair as a Mechanism of Resistance to *cis*-Diamminedichloroplatinum(II)†

Alan Eastman* and Nancy Schulte

Eppley Institute for Research in Cancer, University of Nebraska Medical Center, Omaha, Nebraska 68105

Received January 19, 1988

ABSTRACT: Murine leukemia L1210 cells, either sensitive or resistant to the toxic action of the cancer chemotherapeutic agent *cis*-diamminedichloroplatinum(II), have been studied for potential differences in the formation and repair of drug-induced DNA damage. The sensitivity for these experiments was obtained by using the radiolabeled analogue [^{3}H]-*cis*-dichloro(ethylenediamine)platinum(II). The resistant cells demonstrated a 40% reduction in drug accumulation but a qualitatively similar profile of DNA-bound adducts. These adducts resembled those previously characterized in pure DNA and represented intrastrand cross-links at GG, AG, and GNG (N is any nucleotide) sequences in DNA. Repair of these cross-links occurred in a biphasic manner: rapid for the first 6 h and then much slower. The resistant cells removed up to 4 times as many adducts during the rapid phase of repair. The extent of this repair did not directly correlate with the degree of resistance in that cells with 100-fold resistance were only slightly more effective at repair than cells with 20-fold resistance. Therefore, although enhanced DNA repair is thought to contribute markedly to drug resistance, other mechanisms for tolerance of DNA damage may also occur in these cells.

Development of resistance to cancer chemotherapeutic agents is a major limitation to the clinical use of these drugs. Many experimental cell systems have been developed to investigate the potential mechanisms of resistance to *cis*-diamminedichloroplatinum(II) (*cis*-DDP)[1] [reviewed in Eastman and Richon (1986)]. Various patterns of cross-resistance have been reported. Cells may be either specifically resistant to *cis*-DDP or also cross-resistant to other alkylating agents or even cadmium. In the latter cases, alterations in glutathione or metallothionein levels have been implicated in the resistance mechanism.

In the past year, a number of reports have suggested that reduced accumulation of *cis*-DDP may contribute, albeit only partially, to the mechanism of resistance (Kraker et al., 1986; Hromas et al., 1986; Andrews et al., 1986). This laboratory demonstrated that murine leukemia L1210 cells preferentially resistant to *cis*-DDP (L1210/DDP) have a slightly reduced accumulation of drug but the major contribution to resistance occurs after DNA is platinated (Richon et al., 1987).

DNA is believed to be the critical biological target (Roberts & Thomson, 1979). Damage in the form of specific DNA adducts has been characterized (Eastman, 1983, 1986; Fichtinger-Schepman et al., 1985). The major adducts are DNA intrastrand cross-links, but the DNA interstrand cross-links that represent less than 1% of the total platination have more often been implicated as the most cytotoxic lesions [reviewed in Eastman (1987a)]. In bacteria, sensitivity to *cis*-DDP can arise by a deficiency in repair of the damaged DNA (Drobnik et al., 1973; Beck & Brubaker, 1973). Additionally, Sancar and Rupp (1983) showed that the *Escherichia coli* uvrABC excinuclease complex can excise *cis*-DDP adducts from DNA in vitro. A deficiency in cellular repair processes in mammalian cells also contributes to sensitivity to DNA-damaging agents (Fraval et al., 1978; Meyn et al., 1982). The corollary that sensitivity to DNA damage is associated with deficient DNA repair does not hold for every cell line (Rawlings & Roberts, 1986). Thus, DNA repair processes are important determinants of the cytotoxic effects of DNA-damaging agents. However, neither in bacteria nor in mammalian cells has an increase in DNA repair capability been reported as a mechanism of resistance to genotoxic agents.

In the present study, we have investigated potential differences in DNA repair in L1210/0 (sensitive) and L1210/DDP cell lines. These experiments involved analyzing the formation and repair of specific DNA intrastrand cross-links. The sensitivity for these experiments was obtained by using [^{3}H]-*cis*-dichloro(ethylenediamine)platinum(II) ([^{3}H]-*cis*-DEP), an analogue of *cis*-DDP that produces adducts at identical sites in DNA [reviewed in Eastman (1987a)] and

† Supported by National Cancer Institute Research Grants CA36039 and CA00906 and Cancer Center Support Grant CA36727.
* Address corresponendence to this author.

[1] Abbreviations: *cis*-DDP, *cis*-diamminedichloroplatinum(II); *cis*-DEP, *cis*-dichloro(ethylenediamine)platinum(II); HPLC, high-pressure liquid chromatography; Tris, tris(hydroxymethyl)aminomethane; EDTA, ethylenediaminetetraacetic acid.

0006-2960/88/0427-4730$01.50/0